EFDA–JET–PR(08)43

F. Zonca, L. Chen, A. Botrugno, P. Buratti, A. Cardinali, R. Cesario,
V. Pericoli Ridolfini and JET EFDA contributors

High-Frequency Fishbones at JET: Theoretical Interpretation of Experimental Observations

High-Frequency Fishbones at JET: Theoretical Interpretation of Experimental Observations

F. Zonca[1], L. Chen[2, 3], A. Botrugno[1], P. Buratti[1], A. Cardinali[1], R. Cesario[1], V. Pericoli Ridolfini[1] and JET EFDA contributors*

JET-EFDA, Culham Science Centre, OX14 3DB, Abingdon, UK

[1]Associazione EURATOM-ENEA sulla Fusione, C.P. 65 - I-00044 - Frascati, Italy
[2]Department of Physics and Astronomy, Univ. of California, Irvine CA 92697-4575, U.S.A.
[3]Institute for Fusion Theory and Simulation, Zhejiang University, Hangzhou 310027, P.R.C.
** See annex of F. Romanelli et al, "Overview of JET Results",*
(Proc. 22[nd] IAEA Fusion Energy Conference, Geneva, Switzerland (2008)).

Preprint of Paper to be submitted for publication in
Nuclear Fusion

ABSTRACT

The existence of fishbone fluctuations at frequencies comparable with those of Geodesic Acoustic Modes (GAM) and Beta induced Alfvén Eigenmodes (BAE) has been demonstrated theoretically in a recent work [Nucl. Fusion **47** (2007) 1588]. Here, we show that observation of fishbones at unexpectedly high frequencies in JET [Phys. Plasmas **12** (2005) 102509] is well interpreted as experimental evidence of high (GAM/BAE range) frequency fishbones and discuss the insights concerning both supra-thermal particles as well as thermal plasma properties that can be obtained from experimental observations.

INTRODUCTION

The relationship of MHD and low frequency fluctuations of the shear Alfvén wave (SAW) spectrum with micro-turbulence has important implications for the long time scale dynamic behaviors in burning plasmas [1, 2, 3, 4, 5]. In the Kinetic Thermal Ion (KTI) frequency gap of the SAW continuous spectrum [2], i.e. at frequencies of the order of the thermal ion transit frequency, all these phenomena occur on similar time scales, facilitating cross-scale couplings and enhancing their mutual interactions via a direct link between drift-wave turbulence (DWT), zonal flows (ZF) [6] and Geodesic Acoustic Modes (GAM) [7] on the one side and the SAW spectrum on the other, driven by both energetic as well as thermal particles. Examples of such interactions are plasma nonlinear behaviors, which occur due to mediation by zonal structures, i.e. the nonlinear equilibria [8] that are formed, e.g., by ZF [6], zonal fields [9, 10, 11], and radial corrugations of equilibrium profiles [1, 12]. Other examples that have been recently explored [5] are connected with the close relationship between GAM and SAW spectra [13, 14].

In this work, we explore one particular evidence of the relationship of MHD and low frequency fluctuations of the SAW spectrum, i.e. the existence of fishbone fluctuations at frequencies comparable with those of GAM and Beta induced Alfvén Eigenmodes (BAE) [15, 16]. The possibility of exciting fishbone oscillations in the GAM/BAE frequency range was demonstrated analytically [17, 18], but no clear experimental evidence confirming theoretical expectations has been reported so far. Experimental observation if this phenomenology would be important since it would provide an element of verification for the conceptual framework describing the MHD/SAW/DWT interplay mentioned above. Here, we demonstrate that observation of fishbones at unexpectedly high frequencies in JET [19] is well interpreted as experimental evidence of fishbone oscillations in the GAM/BAE frequency range [18]. In the given theoretical framework [18], we also show that, from the mere observation of the fluctuation frequency spectrum, quantitative information can be obtained concerning both supra-thermal particles as well as thermal plasma properties.

The plan of the paper is as follows. In Section 2, we present the general theoretical framework and describe the dispersion relation for high frequency fishbones. Experimental observation of high frequency fishbones at JET is analyzed in Section 3 for JET pulse # 54300 [19], while theo-

retical interpretations are discussed in Section 4. Finally, Section 5 is devoted to conclusions and discussions.

GENERAL FISHBONE DISPERSION RELATION AND HIGH FREQUENCY FISHBONES

Perturbations of the SAW spectrum generally consist of singular (inertial) and regular (ideal MHD) structures. For this reason, via asymptotic analyses it is always possible to derive a general *fishbone-like* dispersion relation in the form [2, 3, 18, 20, 21, 22]

$$i\Lambda(\omega) = \delta\tilde{W}_f + \delta\tilde{W}_k \quad . \tag{1}$$

Here, $i\Lambda(\omega)$ is the inertial layer contribution due to thermal ions, while the right hand side comes from background MHD and Energetic Particle (E.-P.) contributions in the regular ideal regions. In particular, Alfvén Eigenmode (AE) collective excitations by E.-P. are possible due to the coupling of the E.-P. pressure perturbation with the SAW vorticity equation via magnetic curvature drifts [22]. An expression formally similar to Eq. (1) has been recently derived for BAE by Nguyen et al. using a variational formulation [23].

In the banana regime, $|\omega| \ll \omega_{bi}$, with ω_{bi} the (magnetically trapped) thermal ion bounce frequency, the asymptotic expression of Λ is given by [24]

$$\Lambda^2 = \left(\omega^2/\omega_A^2\right)\left(1-\omega_{*pi}/\omega\right)\left[1+\left(1.6(R_0/r)^{1/2}+0.5\right)q^2\right] \quad , \tag{2}$$

where $\omega_A = v_A/qR_0$, v_A denotes the Alfvén speed, q the safety factor, R_0 the torus major radius, r the radial flux coordinate (minor radius), $\omega_{*pi} = (T_i c/eB)(\mathbf{k}\times\mathbf{b})\cdot\nabla P_i/P_i$, $\mathbf{b}\equiv\mathbf{B}/B$, $\mathbf{k}$ is the wave-vector and other symbols are standard. Meanwhile, in the high-frequency regime $\omega_{ti} \ll |\omega| \ll \omega_A$, with $\omega_{ti} = (2T_i/m_i)^{1/2}/(qR_0)$ the thermal ion transit frequency [18, 25],

$$\Lambda^2 = \frac{\omega^2}{\omega_A^2} - \frac{\omega_{BAE}^2}{\omega_A^2}\left[1+\frac{\omega_{BAE}^2}{q^2\omega^2}\frac{(46/49)+(32/49)(T_e/T_i)+(8/49)(T_e/T_i)^2}{\left(1+(4/7)(T_e/T_i)\right)^2}\right] , \tag{3}$$

with $\omega_{BAE} = q\omega_{ti}(7/4+T_e/T_i)^{1/2}$ being the asymptotic expression of the BAE [15, 16] accumulation point of the SAW continuous spectrum in the fluid limit [25, 26, 27, 28, 29]. The general kinetic expression of Λ (Λ is generally complex) for $\omega_{bi} < |\omega| \ll \omega_A$ is given in Ref. [25, 26, 28]

$$\Lambda^2 = \frac{\omega^2}{\omega_A^2}\left(1-\frac{\omega_{*pi}}{\omega}\right) + q^2\frac{\omega\omega_{ti}}{\omega_A^2}\left[\left(1-\frac{\omega_{*ni}}{\omega}\right)F(\omega/\omega_{ti}) - \frac{\omega_{*Ti}}{\omega}G(\omega/\omega_{ti}) - \frac{N^2(\omega/\omega_{ti})}{D(\omega/\omega_{ti})}\right] , \tag{4}$$

where $\omega_{*ni} = (T_i c/eB)(\mathbf{k}\times\mathbf{b})\cdot(\nabla n_i)/n_i$, $\omega_{*Ti} = (T_i c/eB)(\mathbf{k}\times\mathbf{b})\cdot(\nabla T_i)/T_i$ and the functions, $F(x)$, $G(x)$, $N(x)$ and $D(x)$ are defined as $F(x) + x\left(x^2+3/2\right) + \left(x^4+x^2+1/2\right)Z(x)$, $G(x) = x\left(x^4+x^2+2\right) + \left(x^6+x^4/2+x^2+3/4\right)Z(x)$, $N(x) = \left(1-\omega_{*ni}/\omega\right)\left[x+\left(1/2+x^2\right)Z(x)\right] - \left(\omega_{*Ti}/\omega\right)\left[x\left(1/2+x^2\right)+\left(1/4+x^4\right)Z(x)\right]$, $D(x) = (1/x)\left(1+T_i/T_e\right) + \left(1-\omega_{*ni}/\omega\right)Z(x) - \left(\omega_{*Ti}/\omega\right)\left[x+\left(x^2-1/2\right)Z(x)\right]$, with $Z(x) = \pi^{-1/2}\int_{-\infty}^{\infty} e^{-y^2}/(y-x)dy$ the plasma dispersion function.

The shear Alfvén continuous spectrum is described by $\Lambda^2 = k_\parallel^2 q^2 R_0^2$ [25] for $|k_\parallel| qR_0 \ll 1$. Thus, the shear Alfvén frequency gap is given by the condition $\mathbb{R}\mathrm{e}\Lambda^2 < 0$ and, on the basis of

this dispersion relation, Eq. (1), two types of modes exist [2, 3, 22]: a discrete Alfvén Eigenmode (AE), for $\mathbb{R}\mathrm{e}\Lambda^2 < 0$; and an Energetic Particle continuum Mode (EPM) [21] for $\mathbb{R}\mathrm{e}\Lambda^2 > 0$. The combined effect of $\delta\tilde{W}_f$ and $\mathbb{R}\mathrm{e}\delta\tilde{W}_k$, which determines the existence conditions of AE by removing the degeneracy with the SAW accumulation point, depends on the plasma equilibrium profiles. Thus, various effects in $\delta\tilde{W}_f + \mathbb{R}\mathrm{e}\delta\tilde{W}_k$ can lead to AE localization in various gaps, i.e. to different species of AE [2, 3]. This AE Zoology [30] is consistently described by the single and general dispersion relation, Eq. (1), which accounts for the resonant excitation of the SAW frequency spectrum by energetic and thermal ions in the range $\omega_{*pi} \approx \omega_{ti} \lesssim \omega \ll \omega_A$ [22], i.e. from the low Kinetic Ballooning Mode (KBM) [20, 31, 32] and BAE [15, 16] frequency up to the higher frequency typical of toroidal AEs (TAEs) [33, 34, 35]. Note that the expression of Λ depends only on physical quantities that determine wave-particle dynamics in the singular kinetic (inertial) layer and, thus, never depends on equilibrium parameters such as magnetic shear $s = r(dq/dr)$. For this reason and without loss of generality, we have written Eq. (1) for finite s, which is the relevant case for the present analysis; its straightforward extensions to $s = 0$ are discussed in Refs. [2, 18, 22, 36, 37]. In the case of EPM, meanwhile, ω is set by the relevant energetic ion characteristic frequency and mode excitation requires the drive exceeding a threshold due to continuum damping [38, 39, 40, 41, 42]; i.e., $\mathbb{I}\mathrm{m}\delta\tilde{W}_k > \mathbb{R}\mathrm{e}\Lambda$ [20, 21, 43] in Eq. (1).

Since singular structures characterizing the SAW spectrum are independent of the mode number except for a scale factor, Eq. (1) applies to macroscopic MHD modes as well [44], including $(n, m) = (1, 1)$ fishbone oscillations [45], with n/m the toroidal/poloidal mode number. When considering kinetic effects on low mode number MHD modes, sideband poloidal mode numbers cannot be considered degenerate and the expression of Λ in Eq. (4) is replaced by

$$\Lambda^2 = \frac{\omega^2}{\omega_A^2}\left(1 - \frac{\omega_{*pi}}{\omega}\right) + q^2\frac{\omega\omega_{ti}}{\omega_A^2}\left[\left(1 - \frac{\omega_{*ni}}{\omega}\right)F - \frac{\omega_{*Ti}}{\omega}G - \frac{N_m}{2}\left(\frac{N_{m+1}}{D_{m+1}} + \frac{N_{m-1}}{D_{m-1}}\right)\right] . \qquad (5)$$

Here, the dependence on $x = \omega/\omega_{ti}$ of the functions $F(x)$, $G(x)$, $N_m(x)$ and $D_m(x)$ is implicitly assumed, while $N_m(x)$ and $D_m(x)$ are defined as the functions $N(x)$ and $D(x)$ given above, having made explicit the poloidal mode number m to be used for computing their dependences on diamagnetic frequencies. Note that Eq. (5) reduces to Eq. (4) at either $|m| \gg 1$ or for negligible diamagnetic effects as, e.g., in Ref. [46]. Here, the most general form is retained for completeness. Equation (5) is readily derived [47] considering that ballooning formalism is a particular limiting case of a more general mode structure decomposition based on the Poisson Summation Formula [48]. The necessity of considering the degeneracy removal between poloidal sidebands parallel wave-vectors for finite $|k_\parallel|qR_0$ has been recently noted by Lauber et al. in analyzing BAE modes in Asdex Upgrade [49] and by Gorelenkov et al. in kinetic analyses of the Beta induced Alfvén Acoustic Eigenmode continuum [50, 51]. Here, this further extension of Eq. (5) is unneeded, for we are investigating macroscopic MHD modes with inertial/kinetic layer at $k_\parallel qR_0 = 0$.

From the structure of Eq. (1), we can expect that very near marginal stability and for weak drive, modes of the SAW spectrum are located in the neighborhood of the SAW accumulation point at

$\Lambda = 0$. In other words, accumulation points are the natural "gateway" through which SAW begin to appear as physical and observable objects for increasing kinetic drive $\delta\tilde{W}_k$ and/or decreasing plasma potential energy $\delta\tilde{W}_f$. The precessional fishbones [43] are the first and notable example of EPM [2, 3], while diamagnetic fishbones [52] are the analogue of AE. Following the original reference for both physics model and notation, the fishbone dispersion relation [43, 52] is obtained for $\delta\tilde{W}_f = \delta\hat{W}_f/|s|$, $\delta\tilde{W}_k = \delta\hat{W}_k/|s|$, where

$$\delta\hat{W}_f = 3\pi\Delta q_0 \left(13/144 - \beta_{ps}^2\right)\left(r_s^2/R_0^2\right) \tag{6}$$

is the simplest expression given by [53], with $\beta_{ps} = -(R_0/r_s^2)^2 \int_0^{r_s} r^2 (d\beta/dr) dr$, r_s the $q(r_s) = 1$ radius, $\Delta q_0 = 1 - q(r=0)$, $\beta = 8\pi P/B_0^2$ the ratio of kinetic and magnetic pressures and B_0 the on-axis equilibrium magnetic field. The fluid term, $\delta\hat{W}_f$, includes the contribution of the energetic (hot) particle adiabatic and convective responses as well [43]. Meanwhile, the kinetic $\delta\hat{W}_k$ is [43]

$$\delta\hat{W}_k = 4\frac{\pi^2}{B_0^2} M\omega_c^2 \frac{R_0}{r_s^2} \int_0^{r_s} \frac{r^3}{q} dr \int \mathcal{E} d\mathcal{E} d\lambda \sum_{v_\parallel/|v_\parallel|=\pm 1} \overline{e^{\mathrm{i}q(r)\theta}\omega_d e^{-\mathrm{i}\theta}}\, \overline{e^{\mathrm{i}\theta}\omega_d e^{-\mathrm{i}q(r)\theta}} \frac{\tau_b Q F_0}{\bar{\omega}_d - \omega} \quad , \tag{7}$$

where M is the energetic particle mass, $\omega_c = (eB/Mc)$ is the cyclotron frequency, $\mathcal{E} = v^2/2$, $\lambda = \mu B_0/\mathcal{E} = (B_0/B)v_\perp^2/v^2$, $\mathbf{B}\cdot\nabla(\zeta - q(r)\theta) = 0$, ζ is the "toroidal angle" chosen such that (r, θ, ζ) is a toroidal flux coordinate system with straight field lines ($q = q(r)$), $\overline{(...)} = (\oint v_\parallel^{-1} d\ell)^{-1} \oint v_\parallel^{-1}(...) d\ell$ denotes bounce-averaging, ℓ is the arc length along the equilibrium $\mathbf{B}$-field, τ_b is the bounce/transit time for magnetically trapped/circulating particles, ω_d is the magnetic drift frequency and $QF_0 = (\omega\partial_\mathcal{E} + \hat{\omega}_*)F_0$, $\hat{\omega}_* F_0 = \omega_c^{-1}(\mathbf{k}\times\mathbf{B}/B)\cdot\nabla F_0$, with $F_0 = F_0(\mathcal{E}, \lambda, v_\parallel/|v_\parallel|)$ the fast particle equilibrium distribution function. With these definitions, Eq. (1) describes fishbone excitations by energetic ions [43, 45, 52] as well as supra-thermal electrons [18, 54, 55, 56, 57, 58, 59, 60, 61, 62]. In the case of fast ion excitation, Eq. (7) must be corrected for energetic ion finite orbit width effects (see, e.g., Ref. [24]).

Usually, fishbone modes excitation is described by Eq. (1) with Λ given by Eq. (2), the precessional fishbone [43] being the EPM while the diamagnetic fishbone [52] playing the role of AE [2, 3]. For weak drive and near marginal stability, these modes are expected to accumulate near $\omega = \omega_{*pi}$, which is usually low frequency in the MHD sense. However, JET experiments with strong ion cyclotron resonance heating (ICRH) only, low-density plasmas and high fast ions energy contents [19] reveal a rich phenomenology, where fishbone frequency clearly accumulates at finite frequency (see Fig. 1). This phenomenon is discussed and interpreted in the next two sections within the present theoretical framework, given by Eq. (1) and Λ from Eqs. (3) and (5). In Ref. [18], we demonstrated that, if the effective temperature of the supra-thermal particle tail is sufficiently high, theory predicts excitation of fishbone oscillations at frequencies comparable to those typical of GAM [7] or BAE [15, 16], which are known to be degenerate [1, 2, 13, 18]. In the same work [18], we also anticipated that high-frequency (GAM/BAE range) fishbone excitation could explain some features of fishbones observed at JET [19].

EXPERIMENTAL OBSERVATION OF HIGH FREQUENCY FISHBONES AT JET

Experimental conditions and qualitative analyses of the fishbones cycle around a monster sawtooth period have been extensively discussed in Ref. [19]. Here, we want to focus on some features that have been previously neglected and, meanwhile, reveal useful insights concerning both supra-thermal particles as well as thermal plasma properties that can be obtained from experimental observations.

We focus on JET pulse # 54300 and, more specifically, on the transition between various fishbone branches shown in Fig. 11 from Ref. [19], which is reproduced in Fig. 1 for the reader's convenience. This pulse belongs to a series of JET experiments on ICRH in deuterium plasmas, characterized by low-density and high fast ions energy contents, which all reveal a rich fishbone phenomenology [19]. It is characterized by $B_0 = 2.7$ T and $I_p = 2.5$ MA. The ICRH scheme is hydrogen minority heating in deuterium plasma. The injected power is 8 MW on 5% hydrogen minority at a frequency of 42.5 MHz and resonant radius of 2.99 m, corresponding to on axis heating since $R_0 = 3.00$ m from EFIT magnetic equilibrium reconstruction.

With this ICRH scheme, sawtooth crashes (monster sawtooth) become infrequent and fishbones develop in a long quiescent phase between two crashes. Figure 1 shows fishbone activity between two sawtooth crashes at 8.68s. and 9.57s. In the time interval $9.1\text{s} < t < 9.3\text{s}$, the $q = 1$ rational surface is at $r_s = 0.31 \pm 0.02$ m as desumed from the observed sawtooth inversion radius in the electron temperature profile, measured by ECE spectrometer (KK3); this value is in good agreement with the equilibrium reconstruction. Electron density is $1.92 \pm 0.06 \times 10^{19}\text{m}^{-3}$ and has been measured by standard LIDAR technique (LIDR/NE). Because of its low acquisition rate, the averaged electron density value on a time-window longer than the time interval of interest has been considered ($8.88\text{s} \leq t \leq 9.63\text{s}$). Electron temperature at the $q = 1$ surface is $T_e(r_s) = 4.9 \pm 0.1$ keV.

The diamagnetic ion frequency has been calculated from the expression following Eq. (2) on the basis of experimental measurements reported above and considering $k_\theta = -m/r_s = -1/r_s$. Assuming $T_i = T_e$ and $n_i = n_e$, we obtain $\omega_{*pi}/2\pi = (\omega_{*ni} + \omega_{*Ti})/2\pi = (1.4 + 2.2)\text{kHz} = 3.6\text{kHz}$ at the $q = 1$ surface, having taken $-R_0\partial_{r_s} \ln n_i = 4.4$ and $\eta_i = \partial \ln T_i/\partial \ln n_i = \eta_e = \partial \ln T_e/\partial \ln n_e = 1.6$ as computed from experimental data by a three-point formula and averaged on the time interval $9.1\text{s} < t < 9.3\text{s}$. No direct measurements of ion temperature are available, for the neutral beam system was not active during pulse # 54300.

The effective (perpendicular) temperature of supra-thermal (hydrogen) minority ions has been calculated using PION code [63], which evaluates the energy density distribution (PION/WD1) and the fast ion density (PION/NF1) by solving a time dependent Fokker-Planck equation including the ICRH power deposition. In this way, we obtained $T_h \lesssim 730$ keV for the perpendicular fast ion tail $\propto \exp(-E_\perp/T_h)$, considering the minority ion pressure in the supra-thermal tail only, i.e., neglecting the energy density of the minority ion species characterized by thermal energies.

Fishbone classification in Ref. [19] defines $(n, m) = (1, 1)$ oscillations at frequencies $\nu \gtrsim 40$

kHz as precessional fishbones, whereas fluctuations at $\nu \lesssim 20$ kHz are indicated as diamagnetic fishbones. A third class of hybrid fishbones is also described, referring to strongly driven modes whose frequency dynamically changes from high ($\nu \gtrsim 40$ kHz) to low frequencies ($\nu \lesssim 20$ kHz) within a single burst [19]. This classification – although legitimate in a broad qualitative sense – does not generally coincide with the more quantitative criterion based on the sign of $\mathbb{R}\mathrm{e}\Lambda^2$ and discussed in Section , which emphasizes the correspondence of precessional fishbones [43] with EPM and of diamagnetic fishbones [52] with AE. In particular, modes at $\nu \gtrsim 40$ kHz may well be AE in the BAE frequency gap, whose existence requires $\delta\tilde{W}_f + \mathbb{R}\mathrm{e}\delta\tilde{W}_k < 0$ [2, 3, 22], rather than EPM, for which $\mathbb{I}\mathrm{m}\delta\tilde{W}_k > \mathbb{R}\mathrm{e}\Lambda$ [20, 21, 43] provides the threshold condition, with Λ given by Eq. (3) or the more precise Eq. (5). Clearly, modes at $\nu \approx 80$ kHz and limited dynamic frequency range may be AE, while modes robustly departing from the BAE accumulation point ($\Lambda = 0$) are EPM; there is no sharp transition between the two branches, as theory demonstrates [2, 3, 20, 21, 22, 43, 64, 65] and experiment has recently confirmed [66]. Similar considerations may be drawn for the lower frequency fluctuations at $\nu \lesssim 20$ kHz. Also in this case, transition from the diamagnetic [52] (AE) to precessional [43] (EPM) fishbones is continuous [67]. In the specific case of Fig. 1, fluctuations are evidently of the EPM type, since their frequency is typically higher than the shear Alfvén continuum accumulation point at $\omega \simeq \omega_{*pi}$ ($\omega = \omega_{*pi}$ when wave-particle kinetic interactions with the thermal plasma are neglected).

A thorough and systematic investigation of the fishbone dispersion relation, Eq. (1), for detailed comparisons with experimental observations is beyond the scope of the present work. In fact, for a fully meaningful comparison of theory vs. experiment one should employ a nonlinear analysis, which is certainly required for explaining such a broad dynamic range of chirping frequencies as that observed in JET experiments [19], especially in connection with the so called hybrid fishbones. Besides, one would need to further extend the expression of Λ, given in Eq. (5), to $\omega_{*pi} \lesssim |\omega| \lesssim \omega_{bi}$ and include trapped thermal ion dynamics for a correct treatment of the SAW continuous spectrum in the whole relevant range of frequencies [68]. Here, our scope is to show that Eqs. (1) to (5) describe the physics of the transition from (using Ref. [19] classification) "hybrid" fishbones to "diamagnetic" fishbones shown in Fig. 11 of [19], reproduced here as Fig. 1. This change of dynamic fishbone regime is qualitatively understood in terms of changes of the supra-thermal particle population, while the background thermal plasma can be assumed as fixed, at least to the leading order. The "hybrid" fishbone activity can be explained with the fact that the dominant resonant fast particle drive is located in the high frequency portion of the spectrum (see next Section). After subsequent "hybrid" fishbone bursts, this frequency domain (corresponding to an energy domain of the fast particle phase space) of strongest resonant drive is depleted and, with weaker fast ion source, either low- or high-frequency modes can be excited, due to the continuous re-building of the ICRH supra-thermal tail. In fact, as the lower frequency fishbones get excited – connected with the ω_{*pi} accumulation point described by Eq. (2) – and less free energy is available for higher frequency mode excitation (modes are less strongly driven), theory predicts that frequency chirping

should decrease and the mode frequency should get closer to the accumulation point. However, this is evidently not the usual accumulation point at $\simeq \omega_{*pi}$, but rather the accumulation point described by Eq. (3). In fact, Fig. 1 shows the frequency accumulation at about 80 kHz. This point is discussed in detail in the next Section, where we show that experimental measurements can be easily used to gain further insights concerning both supra-thermal particles as well as thermal plasma properties; e.g., we show the importance of plasma kinetic effects for a correct determination of the SAW accumulation point and of the quantities that can be inferred from that. In other words, we show the importance of generally using Eq. (5) rather than Eq. (3).

THEORETICAL INTERPRETATION

At high frequencies, $\omega_{ti} \lesssim |\omega| \ll \omega_A$, Eq. (3) applies instead of Eq. (2); thus, the asymmetry of the shear Alfvén continuous spectrum is lost and modes can equally propagate in both ion and electron diamagnetic directions [18]. Equation (3) describes the formation of the BAE [15, 16] spectral gap: so, in addition to ion fishbones, electron fishbones propagating in the electron diamagnetic direction and normal pressure profiles could be excited [18]. For these modes, finite diamagnetic frequency usually provides higher order corrections to the frequency spectrum ($|\omega_*/\omega| \ll 1$ [46]) and Eq. (4) could be used instead of Eq. (5) for computing Λ from kinetic theory; here, we maintain Eq. (5) for generality.

Using JET pulse # 54300 experimental data reported in Section , we find $\omega_{ti}/2\pi = 36\mathrm{kHz}$ at $T_i = T_e$ on the $q = 1$ surface; thus, modes with $\nu \gtrsim 40$ kHz in Fig. 1 must be considered high-frequency modes in the sense discussed in the present work. These modes can be considered as high-frequency fishbones for two main reasons: their mode structure is that typical of $(n, m) = (1, 1)$ internal kinks, resonantly excited by precession resonance with the fast particles [43, 52]; furthermore, for sufficiently strong fast particle drive they are clearly connected with the usual lower frequency fishbones, as shown in Fig. 1. In the weak drive limit, it could be argued that these modes are possibly viewed as $(n, m) = (1, 1)$ BAE for the AE branch. However, as already pointed out, the weakly driven AE branch smoothly connects to the strongly driven EPM branch robustly departing from the BAE accumulation point for increasing supra-thermal particle drive. This point obviously challenges the interpretation of the high-frequency $(n, m) = (1, 1)$ fluctuations as BAE; thus, we use the high-frequency fishbone viewpoint, originally proposed in [17], where these type of oscillations were predicted on the basis of pure theoretical results. In any case, it is important reminding the reader that these nomenclature issues are connected with refined classification aspects of experimentally observed fluctuations, which all fall within the same unified theoretical picture based on the low-frequency shear Alfvén continuous spectrum structure in toroidal geometry [2, 3, 18, 20, 21, 22] [see Eq. (1)].

One crucial condition for effective high-frequency fishbone excitation is that the effective supra-thermal particle tail temperature, T_h, be sufficiently high to allow the fast particle precession frequency to be of the order of the thermal ion transit frequency [18]. Once the mode frequency

ν is known, the value of T_h for optimal mode destabilization can be computed and, vice-versa, given T_h one can determine the mode frequency range for which resonant wave-particle drive is strongest [69, 70]. Estimating the precession frequency with that of deeply trapped particles, resonant wave-particle interactions occur at energy in perpendicular degrees of freedom [18]

$$E_{\perp,\text{eff}}[\text{keV}] \sim 6.30\nu[\text{kHz}]B[\text{T}]R_0^2[\text{m}](r_s/R_0)(nq)^{-1} \quad . \tag{8}$$

For given fast ion distribution, described by a nearly Maxwellian supra-thermal tail, $\propto \exp(-E_\perp/T_h)$ with density n_h, the relationship between ν and T_h can be approximately given by [18]

$$T_h[\text{keV}] \sim (2/5)E_{\perp,\text{eff}} \sim 2.52\nu[\text{kHz}]B[\text{T}]R_0^2[\text{m}](r_s/R_0)(nq)^{-1} \quad . \tag{9}$$

This latter condition can be understood as the definition of the mode frequency at which the resonant wave-particle drive is strongest [69, 70]. Note that the origin of the $(2/5)$ factor relating $E_{\perp,\text{eff}}$ with T_h is connected with the $\propto {E_\perp}^{5/2} \exp\left(-E_\perp/T_h\right)$ functional dependence on $E_\perp \simeq E$ at the numerator of the integrand in the resonant integral of Eq. (7)[1]. Weaker dependences on E due to QF_0 can cause readjustments of the $(2/5)$ factor [69, 70]; however, the scope here is to give a simple yet relevant lowest order estimate for T_h. This estimate is robust, for it captures the essential ingredients of wave-particle toroidal precession resonance, and provides a lower bound for $E_{\perp,\text{eff}}$, since precession frequency is maximized for deeply trapped particles. For nearly single-pitch angle particle distributions, as in the ICRH case, one can improve Eqs. (8) and (9) by dividing the r.h.s. by the reduction factor of the effective precession frequency with respect to the deeply trapped particle reference value.

Given n_h, T_h and the relationship – Eq. (8) – between ν and $E_{\perp,\text{eff}}$, which is set by the wave-particle resonance condition, $\mathbb{I}\text{m}\delta\hat{W}_k$ decreases exponentially for (high) frequencies such that $T_h < (2/5)E_{\perp,\text{eff}}$, while it decreases algebraically for (low) frequencies corresponding to $T_h > (2/5)E_{\perp,\text{eff}}$. Using characteristic values of JET pulse # 54300, Eq. (9) predicts that $T_h \sim 440$ keV is needed for bringing the $\mathbb{I}\text{m}\delta\hat{W}_k$ exponential (high) frequency cut-off at $\nu \simeq 70$ kHz [2]. This fact explains why high-frequency fishbones cannot be observed unless the supra-thermal tail temperature is sufficiently high. The estimate $T_h \sim 440$ keV for the supra-thermal tail temperature needed for an exponential frequency cut-off at $\nu \gtrsim 70$ kHz agrees well with the value of $T_h \lesssim 730$ keV, computed by the PION code [63] for experimental conditions of JET pulse # 54300, as discussed in Section . Equation (8), meanwhile, gives $E_{\perp,\text{eff}} \sim 1.1$ MeV for most effective wave-particle resonant interactions of a $\nu \simeq 70$ kHz mode with the supra-thermal particle tail. This result compares well with the value of ~ 1 MeV reported in Ref. [19] as computed by the CASTOR-K code [71]. These discussions demonstrate that the present theoretical framework helps quantitatively speculating on fast particle (ion and electron) distribution properties - from the effective tail temperature to the energy of most effective wave-particle resonant interactions - on the basis of the

[1] For a perpendicular injected beam, the strongest wave-particle interactions occur at maximum beam energy E_m; thus, $E_{\perp,\text{eff}} = E_m$ [43].

[2] The value $\nu \simeq 70$ kHz is chosen for simplifying a direct comparison with Ref. [19]. At $\nu \simeq 80$ kHz, as suggested by Fig. 1, Eq. (9) predicts that $T_h \sim 510$ keV.

mere information provided by the wave frequency spectrum. In particular, the estimate for $E_{\perp,\mathrm{eff}}$ is very robust, being related with the wave-particle precession resonance condition. Both $E_{\perp,\mathrm{eff}}$ and T_h expressions can be applied to a wide class of modes, as recently shown in connection with TAE mode destabilization by supra-thermal electron tails in Alcator C-MOD [72]. Ref. [72], in particular, emphasizes the importance of using Lower Hybrid Current Drive (LHCD) in the early phase of the plasma discharge to simultaneously have perpendicular supra-thermal electron tails [18] as well as high-q, which makes it possible to excite high frequency modes (TAE range) at the typical ($T_h \sim 30$ keV) supra-thermal electron temperature. This remark is important from the plasma operation point of view, since it opens the possibility of investigating a wide class of fast-electron driven high-frequency modes belonging to the SAW spectrum, which otherwise would be obtainable only via fast-ion excitations that are more easily accelerated to $T_h \approx 500$ keV, as in the JET pulse # 54300.

To demonstrate that the observation of high frequency precessional fishbones with ICRH in JET [19] can be interpreted as evidence of fishbone excitation at the GAM/BAE frequency, as predicted by theory, we have computed the BAE/GAM accumulation point at the $q = 1$ surface in two ways: (a) via the simplified expression $\omega_{BAE} = q\omega_{ti}(7/4 + T_e/T_i)^{1/2}$, readily derivable from the lowest order solution of Eq. (3); and (b) via numerical solution of $\Lambda = 0$, with Λ given by Eq. (5), i.e. including both thermal ion transit resonances (for the ion Landau damping evaluation) as well as diamagnetic effects (finite ω_{*pi}). For the JET discharge # 54300, we have taken $T_e = 4.9$ keV, $R_0 = 3$ m and $\eta_i = \partial \ln T_i/\partial \ln n = 1.6$ as fixed parameters at $r = r_s$, obtaining the results reported in Table 1. Values of Landau damping are typically small and the difference between using Eq. (4) rather than Eq. (5) is minimal, confirming the sound foundation of neglecting finite sideband mode numbers for $|\omega_*/\omega| \ll 1$ [46]. Meanwhile, comparisons of theoretical frequencies with the experimental value of $\simeq 80$ kHz suggest that a realistic estimate for T_i at the $q = 1$ surface is $T_i \simeq 4.5$ keV with $\omega_{*pi}/2\pi \simeq 3.2$ kHz, in agreement with TRANSP [73] simulations based on experimental data reported in Section , which are the only available term of reference in the absence of direct T_i measurements on JET pulse # 54300. These values are also consistent with those reported in Ref. [19], where the higher diamagnetic frequency values 10 kHz $\lesssim \omega_{*pi}/2\pi \lesssim 20$ kHz are obtained just before a monster sawtooth crash [19].

The good agreement of theoretical predictions with experimental observations confirms the sound basis of the proposed interpretation of high frequency precessional fishbones observed in JET [19] with ICRH as evidence of fishbone excitation at the GAM/BAE frequency [17, 18]. The scaling of the BAE accumulation point frequency with T_e/T_i can be used for diagnostics purposes, similar to the approach proposed in Ref. [29] for Alfvén Cascades. Actually, the results presented here (see Table 1), show that a better evaluation of the accumulation point frequency – and, thus, of the experimental quantities that can be inferred from MHD spectrometry measurements – can be obtained by solving $\Lambda = 0$ from Eq. (5) rather than using $\omega = \omega_{BAE}$ [29], with the additional advantage of computing ion Landau damping of the observed modes as well. This information on

T_i	ω_{*ni}/ω_{ti}	$\omega_{*pi}/2\pi$	$\omega_{BAE}/2\pi$	$\omega_{\Lambda=0}/\omega_{ti}$	γ/ω_{ti}	$\omega_{\Lambda=0}/2\pi$
3.0000	0.029381	2.1727	52.316	2.4807	-0.09404	70.556
3.2000	0.030344	2.3175	53.210	2.4539	-0.10203	72.083
3.4000	0.031278	2.4624	54.090	2.4300	-0.10959	73.578
3.6000	0.032185	2.6072	54.955	2.4086	-0.11679	75.044
3.8000	0.033067	2.7521	55.807	2.3892	-0.12361	76.479
4.0000	0.033926	2.8969	56.647	2.3717	-0.13010	77.892
4.2000	0.034764	3.0418	57.474	2.3558	-0.13626	79.280
4.4000	0.035582	3.1866	58.289	2.3412	-0.14211	80.643
4.6000	0.036381	3.3314	59.093	2.3278	-0.14768	81.983
4.8000	0.037164	3.4763	59.886	2.3155	-0.15298	83.304
5.0000	0.037930	3.6211	60.669	2.3041	-0.15802	84.603
5.2000	0.038681	3.7660	61.442	2.2936	-0.16284	85.886
5.4000	0.039418	3.9108	62.205	2.2838	-0.16743	87.148
5.6000	0.040142	4.0557	62.959	2.2746	-0.17181	88.389
5.8000	0.040852	4.2005	63.704	2.2661	-0.17600	89.618
6.0000	0.041550	4.3454	64.441	2.2582	-0.18000	90.832

Table 1: Theoretical values of the BAE accumulation point, $\omega_{\Lambda=0}$ from $\Lambda = 0$ [Eq. 5)], as a function of T_i and $\omega_{*ni} = \omega_{*pi}/(1 + \eta_i)$. Fixed parameters are $B_0 = 2.7$ T, $T_e = 4.9$ keV, $R_0 = 3$ m, $r_s = 0.31$ m, $-R_0\partial_{r_s} \ln n_i = 4.4$ and $\eta_i = 1.6$. Values of ion Landau damping, γ, are also reported. Ion temperature is in keV, while frequencies are given in kHz.

mode damping can in turn be used to speculate on the amount of drive which is needed to excite the modes. Therefore, with experimental measurements of mode frequency it is also possible to draw conclusions on threshold fast particle density for effective mode destabilization in addition to inferring from Eqs. (8) and (9) useful information on effective energy for wave particle interactions and optimal supra-thermal tail temperature for mode excitation. In the case of Alvén Cascades, of course, the accumulation point at $s = 0$ should be evaluated using $\Lambda^2 = k_{\|s}^2 q_s^2 R_0^2$ [25, 74, 75] (provided that $k_{\|s}^2 q_s^2 R_0^2 \ll 1$), with $k_{\|s}$ and q_s the value of the parallel wave-vector and of the safety factor at the minimum-q surface. Note that magnetic shear never enters in the accumulation point expression, as discussed above and as expected for local oscillations of the shear Alfvén continuum [2, 18, 22].

CONCLUSIONS AND DISCUSSIONS

Observation of fishbones at unexpectedly high frequencies on JET [19] is well interpreted as experimental evidence of high (GAM/BAE range) frequency fishbones, recently predicted by theoretical analyses [17, 18]. In this work we discussed the insights concerning both supra-thermal particles as well as thermal plasma properties that can be obtained from experimental data by the mere observation of the fluctuation frequency spectrum.

The high frequency fishbone accumulation point scaling with T_e/T_i can be used for diagnostics purposes as proposed in previous studies [29] and adopting the kinetic expression of the generalized inertia Λ allows more accurate determination of T_i. Meanwhile, from the high frequency fishbone accumulation point one can determine the effective supra-thermal particle tail temperature T_h for optimal mode destabilization and the corresponding energy of resonant wave-particle interaction, $E_{\perp,\text{eff}}$. Vice-versa, given T_h one can determine the mode frequency range for which resonant wave-particle drive is strongest.

The argument on T_h applies to supra-thermal ions as well as electrons and can be used for a broad class of fluctuations driven by toroidal precession resonance wave-particle interactions. Generally $T_h \approx 500$ keV for $nq = 1$ modes, as for high frequency fishbones on JET [19]: this explains why these modes where not observed before. However, the $T_h \propto \nu(nq)^{-1}$ dependence suggests that high frequency modes can be driven by lower T_h values in high-q conditions, such as those obtained in Alcator C-MOD during LHCD in the early current ramp phase, where TAE excitation was observed by perpendicular supra-thermal electron tails with $T_h \sim 30$ keV [72]. These observations open the path to a variety of potentially interesting experiments looking at a broad frequency range of SAW fluctuations excited by both fast electrons and ions via wave-particle precession resonances.

ACKNOWLEDGMENTS

Precious help by Lars-Göran Eriksson on the use of PION output is kindly acknowledged. The authors are also indebted to useful discussions with S.D. Pinches and grateful to F. Nabais, to the

JET Director F. Romanelli and the Nucl. Fusion Editor P.R. Thomas for granting the permission to reproduce Fig. 11 of Ref. [19]. Useful discussions with Ph. Lauber on Eq. (5) and the more general implications of this work are also kindly acknowledged. This work was supported by the Euratom Communities under the contract of Association between EURATOM/ENEA. This work was also supported by the SciDAC Gyrokinetic Simulation of Energetic Particle Turbulence and Transport (GSEP) project, by the U.S. DOE Contract No. DE-AC02-CHO-3073, by the Guangbiao Foundation of Zhejiang University and by the Goal Oriented Training in Theory (GOTiT) EFDA project. The views and opinions expressed herein do not necessarily represent those of the European Commission.

REFERENCES

[1] ZONCA, F., BRIGUGLIO, S., CHEN, L., FOGACCIA, G., HAHM, T.S., MILOVANOV, A.V., and VLAD, G., Plasma Phys. Control. Fusion **48** (2006) B15

[2] CHEN, L., and ZONCA, F., Nucl. Fusion **47** (2007) S727

[3] CHEN, L., Plasma Phys. Control. Fusion **50** (2008) 124001

[4] ZONCA, F., Int. J. Mod. Phys. A **23** (2008) 1165

[5] ZONCA, F., and CHEN, L., "Structures of the low frequency Alfvén continuous spectrum and their consequences on MHD and micro-turbulence", Theory of Fusion Plasmas, AIP Conference Proceedings **1069** (2008) 355

[6] HASEGAWA, A., MACLENNAN, C.G., and KODAMA, Y., Phys. Fluids **22** (1979) 2122

[7] WINSOR, N., JOHNSON, J.L., and DAWSON, J.M., Phys. Fluids **11** (1968) 2448

[8] CHEN, L., and ZONCA, F., Nucl. Fusion **47** (2007) 886

[9] CHEN, L., LIN, Z., WHITE, R.B., and, ZONCA, F., Nucl. Fusion **41** (2001) 747

[10] GUZDAR, P.N., KLEVA, R.G., DAS, A., and KAW, P.K., Phys. Rev. Lett. **87** (2001) 015001

[11] DIAMOND, P.H., ITOH, S.-I., ITOH, K., and HAHM, T.S., Plasma Phys. Control. Fusion **47** (2005) R35

[12] ZONCA, F., BRIGUGLIO, S., CHEN, L., FOGACCIA, G., and VLAD, G., Nucl. Fusion **45** (2005) 477

[13] ZONCA, F., and CHEN, L., Europhys. Lett. **83** (2008) 35001

[14] SMOLYAKOV, A.I., GARBET, X., FALCHETTO, G., and OTTAVIANI, M., Phys. Lett. A **372** (2008) 6750

[15] HEIDBRINK, W.W., STRAIT, E.J., CHU, M.S., and TURNBULL, A.D., Phys. Rev. Lett **71** (1993) 855

[16] TURNBULL, A.D., STRAIT, E.J., HEIDBRINK, W.W., *et al.*, Phys. FLuids B **5** (1993) 2546

[17] ZONCA, F., CARDINALI, A., BURATTI, P., *et al.*, "Collective Effects and Resonant excitation of electron-fishbones in FTU and HL-1M", 8.th Easter Plasma Mtg. on Reconnection and Turbulence in magnetically confined plasmas (Turin, 2003)

[18] ZONCA, F., BURATTI, P., CARDINALI, A., *et al.*, Nucl. Fusion **47** (2007) 1588

[19] NABAIS, F., BORBA, D., MANTSINEN, M., NAVE, M.F.F., and SHARAPOV, S.E., Phys. Plasmas **12** (2005) 102509

[20] TSAI, S.-T., and CHEN, L., phys. Fluids B **5** (1993) 3284

[21] CHEN, L., Phys. Plasmas **1** (1994) 1519

[22] ZONCA, F., and CHEN, L., Plasma Phys. Control. Fusion **48** (2006) 537

[23] NGUYEN, C., GARBET, X., and SMOLYAKOV, A.I., "Variational derivation of the dispersion relation of kinetic coherent modes in the acoustic frequency range in tokamaks", Phys. Plasmas **15** (2008) 112502

[24] GRAVES, J.P., HASTIE, R.J., and HOPCRAFT, K.I., Plasma Phys. Control. Fusion **42** (2000) 1049

[25] ZONCA, F., CHEN, L., and SANTORO, R.A., Plasma Phys. Control. Fusion **38** (1996) 2011

[26] MIKHAILOVSKII, A.B., Nucl. Fusion **13** (1973) 259

[27] MAZUR, V.A., and MIKHAILOVSKII, A.B., Nucl. Fusion **17** (1977) 193

[28] KOTSCHENREUTHER, M., Phys. Fluids **29** (1986) 2898

[29] BREIZMAN, B.N., PEKKER, M.S., SHARAPOV, S.E., *et al.*, Phys. Plasmas **12** (2005) 112506

[30] HEIDBRINK, W.W., Phys. Plasmas **9** (2002) 2113

[31] TANG, W.M., CONNOR, J.W., and HASTIE, R.J., Nucl. Fusion **20** (1980) 1439

[32] BIGLARI, H., and CHEN, L., Phys. Rev. Lett. **67** (1991) 3681

[33] CHENG, C.Z., CHEN, L., and CHANCE, M.S., Ann. Phys. (1985) **161** 21

[34] CHEN, L., Theory of Fusion Plasmas, J. Vaclavik et al. Eds. (Bologna: SIF) (1988) 327

[35] FU, G.Y., and VAN DAM, J.W., Phys. Fluids B **1** (1989) 1949

[36] HASTIE, R.J., HENDER T.C., CARRERAS, B.A., CHARLTON, L.A., and HOLMES J.A., Phys. Fluids **30** (1987) 1756

[37] ZONCA, F., BRIGUGLIO, S., CHEN, L., DETTRICK, S., FOGACCIA, G., TESTA, D. and VLAD, G., Phys. Plasmas **9** (2002) 4939

[38] CHEN, L., and HASEGAWA, A., Phys. Fluids **17** (1974) 1399

[39] HASEGAWA, A., and CHEN, L., Phys. Rev. Lett. **32** (1974) 454

[40] ZONCA, F., and CHEN, L., Phys. Rev. Lett. **68** (1992) 592

[41] ROSENBLUTH, M.N., BERK, H.L., VAN DAM, J.W., and LINDBERG, D.M., Phys. Rev. Lett. **68** (1992) 596

[42] ZONCA, F., and CHEN, L., Phys. Fluids B **5** (1993) 3668

[43] CHEN, L., WHITE, R.B., and ROSENBLUTH, M.N., Phys. Rev. Lett. **52** (1984) 1122

[44] PEGORARO, F., and SCHEP, T.J., Plasma Phys. Control. Fusion **28** (1986) 647

[45] MCGUIRE, K., GOLDSTON, R., BELL, M., *et al.*, Phys. Rev. Lett. **50** (1983) 891

[46] ANNIBALDI, S.V., ZONCA, F., and, BURATTI, P., Plasma Phys. Control. Fusion **49** (2007) 475

[47] ZONCA, F., in Lecture Notes of the "Gyrokinetic Theory and Numerics" high level course of the "Goal Oriented Training in Theory" EFDA project, B.D. Scott (Ed.) (IPP, Garching, Germany, 3 - 14 November, 2008)

[48] ZONCA, F., CHEN, L., and WHITE, R.B., Theory of Fusion Plasmas (Società Italiana di Fisica, Bologna, 2004) J.W. Connor, O. Sauter and E. Sindoni (Eds.) (2004) pp. 3-12

[49] LAUBER, PH., BRÜDGAM, M., BERK, H.L., *et al.*, 35th EPS Conference on Plasma Phys. (Hersonissos, 9 - 13 June 2008) ECA **32** (2008) O-4.030

[50] GORELENKOV, N.N., *et al.*, "Theory and observations of low frequency eigenmodes due to Alfvén acoustic coupling in toroidal fusion plasmas", Fusion Energy 2008, (Proc. 22nd Int. Fusion Energy Conf. Geneva, 2008), IAEA, Vienna (2008), CD-ROM file TH/5-2

[51] GORELENKOV, N.N., VAN ZEELAND, M.A., BERK, H.L., and CROCKER, N.A., "Beta-induced Alfvén-Acoustic Eigenmodes in NSTX and DIII-D Driven by Beam Ions", submitted to Phys. Plasmas (2009)

[52] COPPI, B., and PORCELLI, F., Phys. Rev. Lett. **57** (1986) 2272

[53] BUSSAC, M.N., PELLAT, R., EDERY, D., and SOULÉ, J.L., *et al.*, Phys. Rev. Lett. **35** (1975) 1638

[54] WONG, K.L., CHU M.S., LUCE T.C., *et al.*, Phys. Rev. Lett. **85** (2000) 996

[55] DING, X.T., LIU, YI., GUO, G.C., *et al.*, Nucl. Fusion **42** (2002) 491

[56] ROMANELLI, F., ANGELINI, B., APICELLA, M.L., *et al.*, "Overview of the FTU Results", Fusion Energy 2002 (Proc. 19th Int. Conf. Lyon, 2002), C&S Papers Series No. 19/C, IAEA, Vienna (2003), CD-ROM file OV/4-5 and http://www.iaea.org/programmes/ripc/physics/fec2002/html/fec2002.htm

[57] MAGET, P., IMBEAUX, F., GIRUZZI, G., *et al.*, Nucl. Fusion **46** (2006) 797

[58] PERICOLI-RIDOLFINI, V., ALEKSEYEV, A., ANGELINI, B., *et al.*, "Overview of the FTU Results", Fusion Energy 2006 (Proc. 21st Int. Conf. Chengdu, 2006), STI/PUB/1292, IAEA, Vienna (2007), CD-ROM file OV/3-4 and http://www-naweb.iaea.org/napc/physics/FEC/FEC2006/html/index.htm

[59] YANG, Q., LIU, Y., DING, X.-T., *et al.*, "Overview of HL-2A Experiment Results", Fusion Energy 2006 (Proc. 21st Int. Conf. Chengdu, 2006), STI/PUB/1292, IAEA, Vienna (2007), CD-ROM file OV/4-1 and http://www-naweb.iaea.org/napc/physics/FEC/FEC2006/html/index.htm

[60] CHEN, W., DING, X.-T., LIU, Y., *et al.*, Chin. Phys. Lett. **25** (2008) 3708

[61] MACOR, A., GONICHE, M., ARTAUD, J.F., *et al.*, "Redistribution of Suprathermal Electron due to Fishbone Frequency Jumps", submitted to Phys. Rev. Lett. (2008); also in 35th EPS Conference on Plasma Phys. (Hersonissos, 9 - 13 June 2008) ECA **32** (2008) P-4.062; also in 13th EU-US TTF Workshop (Copenhagen, 1 - 4 September 2008)

[62] CESARIO, R., PANACCIONE, L., MARINUCCI, M., *et al.*, "Fishbone-like internal kink instability driven by supra-thermal electrons on FTU generated by lower hybrid radiofrequency power", Fusion Energy 2008 (Proc. 22nd Int. Conf. Geneva, 2008) file EX/P8-12 and http://www-pub.iaea.org/MTCD/Meetings/FEC2008/ex_p8-12.pdf

[63] ERIKSSON, L.-G., HELLSTEN, T., and WILLÉN, U., Nucl. Fusion **33** (1993) 1037

[64] CHEN, L., and ZONCA, F., Physica Scripta **T60** (1995) 81

[65] ZONCA, F., and CHEN, L., Phys. Plasmas **3** (1996) 323

[66] FREDRICKSON, E.D., BELL, R.E., DARROW, D.S., *et al.*, Phys. Plasmas **13** (2006) 056109

[67] WHITE, R.B., BUSSAC, M.N., and ROMANELLI, F., Phys. Rev. Lett. **62** (1989) 539

[68] CHAVDAROVSKI, I., and ZONCA, F., "Effects of trapped particle dynamics on the structures of low-frequency shear Alfvén continuous spectrum", submitted to Plasma Phys. Control. Fusion (2009)

[69] ZHENG, L.-J., CHEN, L., and SANTORO, R.A., Phys. Plasmas **7** (2000) 2469

[70] ZONCA, F., and CHEN, L., Phys. Plasmas **7** (2000) 4600

[71] BORBA, D., and KERNER, W., J. Comput. Phys. **153** (1999) 101

[72] SNIPES, J.A., PARKER, R.R., PHILLIPS, P.E., *et al.*, Nucl. Fusion **48** (2008) 072001

[73] GOLDSTON, R.J., McCUNE, D.C., TOWNER, H.H., *et al.*, J. Comput. Phys. **43** (1981) 61

[74] ZONCA, F., CHEN, L., SANTORO, R.A., and DONG, J.Q., Plasma Phys. Control. Fusion **40** (1998) 2009

[75] ZONCA, F., CHEN, L., DONG, J.Q., and SANTORO, R.A., Phys. Plasmas **6** (1999) 1917

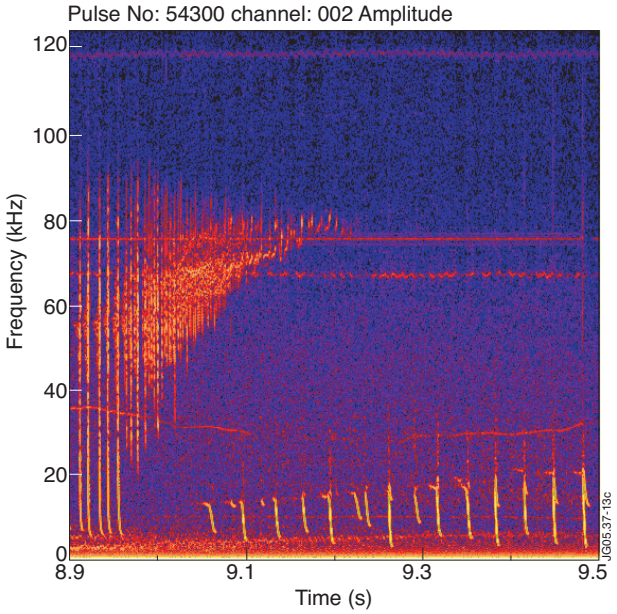

Figure 1: JET Pulse No: 54300. MHD activity from the spectrogram of magnetic coil signal showing the transition to the diamagnetic fishbone regime (Fig. 11, from Ref. [19]). The fishbones accumulating at ~80kHz are the high (GAM/ BAE range) frequency branch discussed in Ref. [18] and in the present work.